Dalton Transactions

Cite this: *Dalton Trans.*, 2012, **41**, 1345

www.rsc.org/dalton

PAPER

Structural organization and dimensionality at the hands of weak intermolecular Au ··· Au, Au ··· X and X ··· X (X = Cl, Br, I) interactions†

Jeffrey S. Ovens, Kimberley N. Truong and Daniel B. Leznoff*

Received 14th September 2011, Accepted 1st November 2011
DOI: 10.1039/c1dt11741f

The salts $K[AuCl_2(CN)_2]\cdot H_2O$ (**1**), $K[AuBr_2(CN)_2]\cdot 2H_2O$ (**2**) and $K[AuI_2(CN)_2]\cdot \frac{1}{3}H_2O$ (**3**) were synthesized and structurally characterized. Compound **1** crystallizes as a network of square planar $[AuCl_2(CN)_2]^-$ anions separated by K^+ cations. However, **2** and **3** feature 2-D sheets built by the aggregation of $[AuX_2(CN)_2]^-$ anions *via* weak, intermolecular X ··· X interactions. The mixed anion double salts $K_3[Au(CN)_2]_2[AuBr_2(CN)_2]\cdot H_2O$ (**4**) and $K_5[Au(CN)_2]_4[AuI_2(CN)_2]\cdot 2H_2O$ (**5**) were also synthesized by cocrystallization of $K[Au(CN)_2]$ and the respective $K[AuX_2(CN)_2]$ salts. Similarly to **2** and **3**, the $[Au(CN)_2]^-$ and $[AuX_2(CN)_2]^-$ anions form 2-D sheets *via* weak, intermolecular $Au^I \cdots X$ and $Au^I \cdots Au^I$ interactions. In the case of **5**, a rare unsupported $Au^I \cdots Au^{III}$ interaction of 3.5796(5) Å is also seen between the two anionic units. Despite the presence of Au(I) aurophilic interactions of 3.24–3.45 Å, neither **4** nor **5** exhibit any detectable emission at room temperature, suggesting that the presence of $Au^I \cdots X$ or $Au^I \cdots Au^{III}$ interactions may affect the emissive properties.

1 Introduction

When designing molecule-based materials, intermolecular interactions can play an important role in the orientation of the constituents and introduce additional dimensionality into a system, thereby impacting the physical properties.[1–17] Intermolecular halogen–halogen (X ··· X; X = Cl, Br, I) interactions are one such type which have been observed in many organic and inorganic solid state materials.[18–21] These are defined by an interatomic distance which is shorter than the sum of their van der Waals radii (3.50 Å for Cl, 3.70 Å for Br and 3.96 Å for I).[22] Such interactions in $[AuBr_2(CN)_2]^-$-containing coordination polymers have been useful in inducing alignment of Br–Au–Br moieties, enhancing optical properties such as birefringence.[16]

Another example of dimensionality-inducing intermolecular interactions are metal-containing systems that contain metallophilic interactions, which are generally restricted to closed-shell metals such as d^{10} Au(I) and Ag(I), $d^{10}s^2$ Tl(I) and Pb(II) and the pseudo closed-shell d^8 Pt(II).[2,4,15,23–28] In particular, Au ··· Au interactions (<3.6 Å) are commonly harnessed in Au(I)-containing materials to increase structural dimensionality. This concept has been exploited extensively with $[Au(CN)_2]^-$-based coordination polymers,[15,29,30] such as in $Zn[Au(CN)_2]_2$, where the changes in $d_{Au–Au}$ (*e.g.* from the uptake of NH_3 vapour) alter the emission properties, allowing this material to function as a sensitive vapour sensor.[31]

In contrast to the aforementioned $Au^I \cdots Au^I$ interactions, the participation of the pseudo closed-shell d^8 Au(III) centre in $Au^I \cdots Au^{III}$ or $Au^{III} \cdots Au^{III}$ aurophilic interactions is much more rarely observed.[2,32–34] For example, in $[Au(C_{14}H_{22}N_4)][AuBr_2]$, a cationic Au(III) centre is observed in close proximity (3.5–3.6 Å interatomic distance) to an anionic Au(I) centre,[35] and $[Au(bipy)Cl_2][AuBr_4]$ contains $Au^{III} \cdots Au^{III}$ contacts of 3.51 Å,[36] however whether these are truly $Au^I \cdots Au^{III}$ or $Au^{III} \cdots Au^{III}$ interactions, or are supported mainly by electrostatic forces remains in question. The explosive $[NMe_4][Au(N_3)_4]$ salt exhibits weak $Au^{III} \cdots Au^{III}$ interactions of 3.507(3)–3.584(3) Å in a 1-D chain of anions, however DFT calculations suggested that in the gas phase, the anions would bind to each other.[37] In other examples, intramolecular Au(I) and Au(III) centres can form interactions, but their proximity is enforced by the binding ligands, as is likely the case for the 3.53 Å $Au^I \cdots Au^{III}$ distance in $[S(Au_2dppf)\{Au(C_6F_5)_3\}_2]$ (dppf = 1,1′-*bis*(diphenylphosphino)ferrocene).[38–41] Although theoretical studies toward better understanding the factors influencing the strength and propensity of these rare interactions to form have been underway,[42,43] there are a distinct lack of examples of materials that exhibit $Au^I \cdots Au^{III}$ interactions unsupported by other stronger forces.

In this light, we herein report the structures of a series of simple potassium salts of the d^8 ion $[AuX_2(CN)_2]^-$ (X = Cl, Br, I); their general syntheses are known,[17,44] but more detailed syntheses are described herein. In addition, the cocrystallization of $[AuX_2(CN)_2]^-$ (X = Br, I) and $[Au(CN)_2]^-$ is shown to generate networks supported by concerts of Au ··· X, $Au^I \cdots Au^I$ and $Au^I \cdots Au^{III}$ interactions.

Department of Chemistry, Simon Fraser University, 8888 University Drive, Burnaby, British Columbia, V5A 1S6, Canada. E-mail: dleznoff@sfu.ca

† CCDC reference numbers 844807–844811. Crystallographic data in CIF format for compounds **1–5**. See DOI: 10.1039/c1dt11741f

2 Experimental

2.1 General procedures and materials

Caution! *Chlorine, bromine and iodine should only be used in a well-ventilated fumehood.*

All reactions were performed in air. $K[AuBr_2(CN)_2]$ was synthesized as previously reported.[17] All other reagents were obtained from commercial sources and used as received.

Infrared spectra were measured with 2 cm^{-1} resolution on a Thermo Nicolet Nexus 670 FT-IR spectrometer equipped with a Pike MIRacle attenuated total reflection (ATR) sampling accessory (4000–700 cm^{-1}). Microanalyses (C, H, N) were performed by Frank Haftbaradaran at Simon Fraser University on a Carlo Erba EA 1110 CHN elemental analyzer.

Solid state luminescence data were collected at room temperature on a Photon Technology International fluorimeter using a Xe arc lamp and a photomultiplier detector. Finely ground powder samples were drop cast from hexanes onto a quartz slide and placed at a *ca.* 22° angle.

2.2 Synthetic procedures

$K[AuCl_2(CN)_2]\cdot H_2O$ (1). This synthesis was based on a literature procedure.[44] Gaseous Cl_2 was bubbled through a 20 mL aqueous solution of $K[Au(CN)_2]$ (1.071 g, 3.717 mmol) for *ca.* 5–10 min, resulting in a yellow tinted solution. Excess Cl_2 was removed by bubbling N_2 through the solution for several minutes, resulting in a colourless solution. Any insoluble impurities were removed by gravity filtration. The solvent was removed by rotary evaporation, leaving a colourless powder of $K[AuCl_2(CN)_2]\cdot H_2O$ (**1**) (1.073 g; 79% yield). Block-shaped X-ray quality crystals were obtained by slow cooling of a heated, saturated ^{i}PrOH solution of **1**. Any remaining impurities can be removed by redissolving **1** in H_2O and gravity filtering the resulting solution. IR (cm^{-1}): 2182 (s; ν_{CN}), 3622 (s), 1605 (s), 741 (w). Anal. calcd for $C_2H_2N_2AuCl_2KO$: C 6.37%, H 0.53%, N 7.43%. Found: C 6.60%, H 0.29%, N 7.45%.

$K[AuI_2(CN)_2]\cdot\frac{1}{3}H_2O$ (3). This synthesis was based on a literature procedure.[44] To a 10 mL methanol solution of $K[Au(CN)_2]$ (106 mg, 0.367 mmol), a 20 mL ethanol solution of I_2 (97 mg, 0.382 mmol) was added, resulting in an intense red solution. This solution was stirred for two hours while covered with aluminum foil. The solvent was removed by rotary evaporation, leaving a brown powder of $K[AuI_2(CN)_2]\cdot\frac{1}{3}H_2O$ (**3**) (172 mg; 86% yield). Needle-shaped X-ray quality crystals were grown by slow evaporation of a methanol solution of **3**. IR (cm^{-1}): 2163 (m; ν_{CN}), 2926 (w), 1630 (m). Anal. calcd for $C_2H_{0.67}N_2AuKI_2O_{0.33}$: C 4.38%, H 0.12%, N 5.11%; Found: C 4.55%, H 0.29%, N 4.87%.

$K_3[Au(CN)_2]_2[AuBr_2(CN)_2]\cdot H_2O$ (4). To a 10 mL methanol solution of $K[Au(CN)_2]$ (28 mg, 0.097 mmol), a 10 mL methanol solution of $K[AuBr_2(CN)_2]$ (39 mg, 0.087 mmol) was added dropwise, resulting in a yellow solution. This solution was partially covered and left to slowly evaporate. Once dry, a mixture of orange needle-shaped crystals of $K_3[Au(CN)_2]_2[AuBr_2(CN)_2]\cdot H_2O$ (**4**) and a yellow powder consisting of starting materials and some AuCN remained. The crystals were isolated manually (10 mg; *ca.* 10% yield). Use of other stoichiometries yielded the same product, but with lower yield. IR (cm^{-1}): 2171 (w; ν_{CN}), 2145 (s; ν_{CN}), 1620 (w). Anal. calcd for $C_6H_2N_6Au_3Br_2K_3O$: C 6.91%, H 0.19%, N 8.06%; Found: C 6.85%, H 0.20%, N 7.49%.

$K_5[Au(CN)_2]_4[AuI_2(CN)_2]\cdot H_2O$ (5). To a 10 mL methanol solution of $K[Au(CN)_2]$ (49 mg, 0.17 mmol), a 10 mL methanol solution of $K[AuI_2(CN)_2]\cdot\frac{1}{3}H_2O$ (22 mg, 0.041 mmol) was added dropwise, resulting in an intense orange solution. This solution was partially covered and left to slowly evaporate. Once dry, a mixture of large red plate-shaped crystals of $K_5[Au(CN)_2]_4[AuI_2(CN)_2]\cdot 2H_2O$ (**5**) and a brown powder consisting of starting materials and some AuCN remained. The crystals were isolated manually (15 mg; *ca.* 23% yield). Use of other stoichiometries yielded the same product, but with lower yield. IR (cm^{-1}): 2168 (w; ν_{CN}), 2144 (s; ν_{CN}), 1606 (m). Anal. calcd for $C_{10}H_4N_{10}Au_5I_2K_5O_2$: C 6.94%, H 0.23%, N 8.09%. Found: C 7.07%, H 0.25%, N 7.89%.

2.3 X-Ray crystallographic analysis

To grow crystals of $K[AuBr_2(CN)_2]\cdot 2H_2O$ (**2**), a minimum amount (less than 1 mL) of boiling H_2O was added to a small amount of $K[AuBr_2(CN)_2]$ and left to slowly cool. Once at room temperature, large yellow needle-shaped crystals of **2** formed. These crystals rapidly desolvate upon removal from the mother liquor. Therefore, **2** was mounted on a MiTeGen sample holder using paratone oil and the data were collected at 150 K. Crystals of **1**, **3**, **4** and **5** were mounted on glass fibres using epoxy adhesive, and the data were collected at room temperature. Additional crystallographic information can be found in Table 1.

All diffraction data were processed with the Bruker Apex II software suite. The structures were solved with Sir92. Subsequent refinements were performed in CRYSTALS.[45]

Compound **2** crystallized as a twin. Twinning was accounted for using Rotax analysis in CRYSTALS.

Diagrams were made using ORTEP-3[46] and POV-ray.[47]

3 Results and discussion

3.1 Synthesis and crystal structures of $K[AuX_2(CN)_2]$ (X = Cl, Br, I) salts

When an aqueous solution of $K[Au(CN)_2]$ reacts with Cl_2 gas, it undergoes oxidative addition to form $K[AuCl_2(CN)_2]\cdot H_2O$ (**1**), readily identified in the IR through a ν_{CN} shift from 2141 cm^{-1} to 2182 cm^{-1}.[44] The oxidation to Au(III) is further indicated by a significant loss of intensity in this IR stretch.[48–50] Our recent structural studies of $[^nBu_4N][AuX_2(CN)_2]$ (X = Br, I) salts have shown that Br···Br and I···I interactions (as defined by their interatomic distances being less than the sum of their van der Waals radii) hold the $[AuX_2(CN)_2]^-$ anions together, forming layers of anions separated by layers of cations.[16] Here, for $K[AuCl_2(CN)_2]\cdot H_2O$, the crystal structure reveals the square planar $[AuCl_2(CN)_2]^-$ anions (with typical Au–C and Au–Cl bonds)[14,49,51,52] to be completely separated from each other; no Cl···Cl interactions exist in this structure.[20,53] There have been very few reports of Cl···Cl interactions, although interactions between Cl and other, larger halogens have been reported.[11,19] Fig. 1 shows the separation of the $[AuCl_2(CN)_2]^-$ anions by K^+ cations. The interatomic distances between the K^+ and N(cyano) moieties of 2.919(6)–2.963(6) Å as well as those between K^+ and

Table 1 Crystallographic data for compounds **1** to **5**

	1	**2**	**3**	**4**	**5**
Empirical formula	$C_2H_2N_2AuCl_2KO$	$C_2H_4N_2AuBr_2KO_2$	$C_3HN_3Au_{1.5}K_{1.5}I_3O_{0.5}$	$C_6H_2N_6Au_3Br_2K_3O$	$C_{10}H_4N_{10}Au_5K_5I_2O_2$
Formula weight (g mol^{-1})	377.02	483.94	821.87	1042.12	1730.34
Crystal system	Monoclinic	Monoclinic	Monoclinic	Triclinic	Triclinic
Space group	$C2/c$	Cc	$P2_1/c$	$P\bar{1}$	$P\bar{1}$
a (Å)	17.345(10)	21.332(4)	4.3182(3)	8.1153(16)	7.3196(6)
b (Å)	7.712(4)	4.2229(4)	24.4306(18)	10.1791(16)	9.8319(8)
c (Å)	6.126(3)	13.474(3)	13.312(1)	12.875(3)	11.5992(9)
α (deg)	90	90	90	70.416(2)	99.936(1)
β (deg)	101.399(6)	117.087(2)	90.850(1)	88.834(2)	92.457(1)
γ (deg)	90	90	90	70.991(1)	111.249(1)
V (Å^3)	803.3(8)	1080.7(4)	1404.21(18)	942.7(3)	761.26(11)
Z	4	4	4	2	1
T (K)	296(2)	150(2)	296(2)	296(2)	296(2)
ρ_{calcd} (g·cm^{-3})	3.100	2.950	3.883	3.664	3.765
μ (mm^{-1})	19.420	21.349	22.682	28.190	26.743
Reflections (all, unique)	4668, 950	1260, 1260	16403, 3363	10973, 4332	8751, 3540
Reflections [$I_0 \geq 2.50\sigma(I_0)$]	671	1060	2253	2960	2746
R_{int}	0.040	0.046	0.062	0.045	0.050
R, R_w [$I_0 \geq 2.50\sigma(I_0)$]^a	0.0191, 0.0269	0.0467, 0.0643	0.0344, 0.0448	0.0328, 0.0436	0.0391, 0.0549
Goodness of fit	0.9723	1.1468	0.9847	1.0811	1.1557

[a] Function minimized: $\Sigma w(|F_o| - |F_c|)^2$, where $w^{-1} = [\sigma^2(F_o) + (nP)^2]$, with $n = 0.02$ for **1**, **3** and **4**, $n = 0.05$ for **2** and $n = 0.03$ for **5**, and where $P = \frac{1}{3}(F_o + 2F_c)$. $R = \Sigma(|F_o| - |F_c|)/\Sigma|F_o|$ and $R_w = [\Sigma w(|F_o| - |F_c|)^2/\Sigma w|F_o|^2]^{\frac{1}{2}}$.

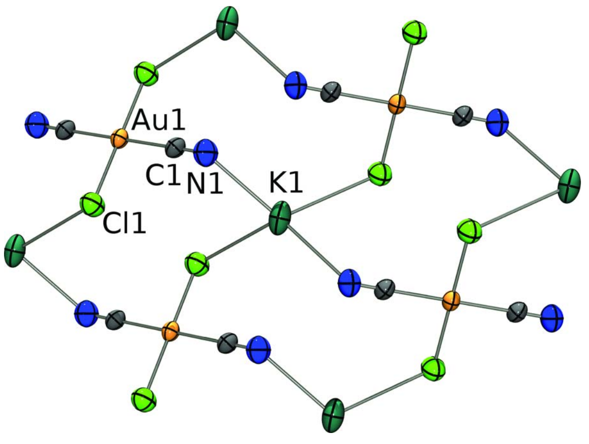

Fig. 1 Crystal structure of **1** showing the separation of $[AuCl_2(CN)_2]^-$ anions by K^+ cations (H_2O molecules not shown). Au, gold; Cl, light green; C, gray; N, blue; K, dark green. Selected bond lengths (Å): Au(1)–Cl(1): 2.2963(18), Au(1)–C(1): 2.036(6), C(1)–N(1): 1.074(7), K(1)–Cl(1): 3.410(3), K(1)–N(1): 2.919(6), K(1)′–N(1): 2.963(6).

Cl of 3.410(3) Å (*cf.* $d_{K–N}$ = 2.75 Å for KCN[54] and $d_{K–Cl}$ = 3.41 Å for KCl[55]) indicate relatively strong interactions between the K^+ cations and the $[AuCl_2(CN)_2]^-$ anions, leaving no room for Cl···Cl interactions.

Similarly, when neat Br_2 is added to an aqueous solution of $K[Au(CN)_2]$, $K[AuBr_2(CN)_2]$ is formed.[17,44] Slow cooling of a saturated H_2O solution of $K[AuBr_2(CN)_2]$ results in the formation of crystals of $K[AuBr_2(CN)_2]\cdot 2H_2O$ (**2**),[48] which rapidly desolvate upon removal from the mother liquor. Fig. 2 shows the $[AuBr_2(CN)_2]^-$ anions forming an overall 2-D sheet by virtue of Br···Br interactions (Table 2). In one dimension, the Br···Br interactions lead to zig-zag chains of $[AuBr_2(CN)_2]^-$ anions ($d_{Br–Br}$ = 3.494(5) Å, *cf.* sum of van der Waals radii for two bromine atoms: 3.70 Å[22]). These chains then interact with each other *via* a different set of Br···Br interactions ($d_{Br–Br}$ = 3.508(4)). Thus, every Br atom is interacting with two other Br atoms to form this network, whereas in the related $[^nBu_4N][AuBr_2(CN)_2]$, only 1-D chains formed *via* pairs of Br···Br interactions. This is likely a factor of the size of the cation.

Table 2 X···X interaction distances (Å) and angles (°) in **2** and **3**

Interaction distances (Å)		Interaction angles (°)	
$K[AuBr_2(CN)_2]\cdot 2H_2O$ (**2**)			
Br(1)–Br(2)	3.494(5)	Au(1)–Br(1)–Br(2)	107.29(16)
Br(1)–Br(2)^a	3.508(4)	Au(1)–Br(1)–Br(2)^a	170.11(16)
$K[AuI_2(CN)_2]\cdot\frac{1}{3}H_2O$ (**3**)			
I(1)–I(2)	3.9296(12)	Au(1)–I(1)–I(2)	112.49(3)
I(1)–I(3)	3.8111(12)	Au(2)–I(3)–I(1)	115.84(3)
I(2)–I(3)	3.8009(12)	Au(2)–I(2)–I(3)	119.26(3)

[a] Symmetry operation: $x, -y, z + 1/2$.

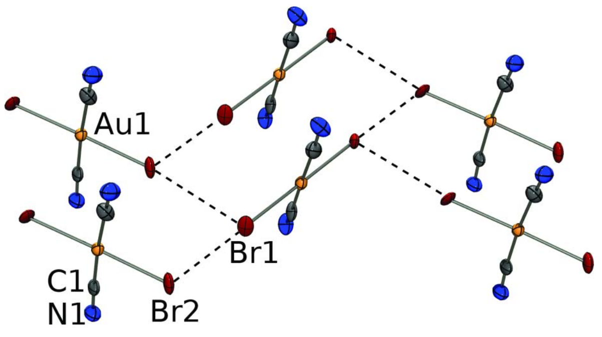

Fig. 2 2-D sheets of **2** formed *via* Br···Br interactions (shown as dashed lines) in two dimensions (K^+ cations and H_2O molecules not shown). Au, gold; Br, scarlet; C, gray; N, blue. Selected bond lengths (Å): Au(1)–Br(1): 2.438(5), Au(1)–Br(2): 2.434(5).

Whereas in **1** the K^+ cations interact with all N(cyano) and chloro moieties, in **2** the K^+ cations solely interact with N(cyano) groups, separating the layers of $[AuBr_2(CN)_2]^-$ anions, as shown in Fig. 3. Approximate interatomic distances (due to poor crystal quality) between K$^+$ and the N(cyano) groups of 2.7–3.2 Å indicate relatively strong interactions.

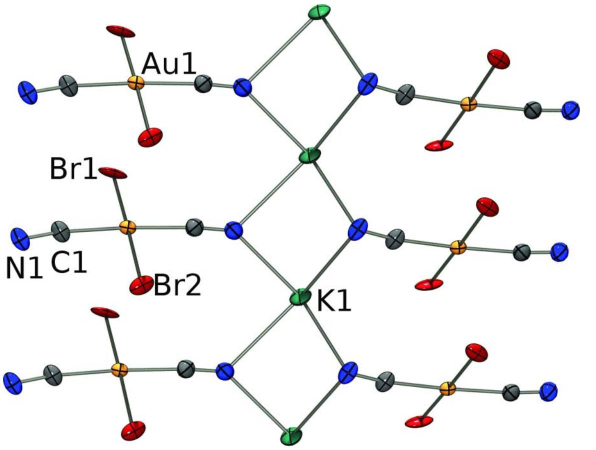

Fig. 3 Layers of $[AuBr_2(CN)_2]^-$ anions are shown separated by K$^+$ cations interacting with the N(cyano) moieties of the $[AuBr_2(CN)_2]^-$ anions. Au, gold; Br, scarlet; C, gray; N, blue; K, dark green. Selected bond lengths (Å; approx.): K–N: 2.7–3.2.

When a stoichiometric ethanol solution of I_2 is added to a methanol solution of K[Au(CN)$_2$], an orange solution forms, from which $K[AuI_2(CN)_2]\cdot\frac{1}{3}H_2O$ (**3**) is isolated. Similar to **1** and **2**, oxidation of Au(I) to Au(III) is observed through a ν_{CN} shift to 2163 cm^{-1}, comparable to the $[^nBu_4N]^+$ salt at 2165 cm^{-1}.[16]

As in **2**, **3** crystallizes as 2-D sheets of $[AuI_2(CN)_2]^-$ anions held together by I···I interactions (Table 2), separated by K$^+$ cations. As shown in Fig. 4, a group of three $[AuI_2(CN)_2]^-$ anions is oriented such that I1, I2 and I3 all have close contacts, forming a triangle of I···I interactions, resulting overall in a 2-D sheet. At $d_{I–I}$ = 3.9296(12) Å, 3.8111(12) Å and 3.8009(12) Å for I1–I2, I1–I3 and I2–I3, respectively, these interactions are all less than the sum of their van der Waals radii (3.96 Å).[22]

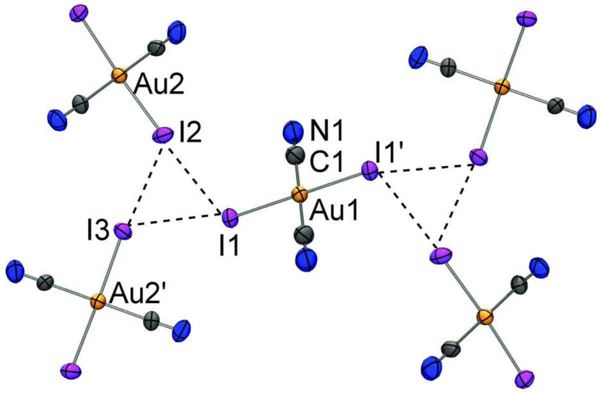

Fig. 4 2-D sheets of **3** formed *via* triangles of I···I interactions (shown as dashed lines; K$^+$ cations and H$_2$O molecules not shown). Au, gold; I, violet; C, gray; N, blue. Selected bond lengths (Å): Au(1)–I(1): 2.6387(8), Au(2)–I(2): 2.6361(10), Au(2)–I(3): 2.6291(9), Au(1)–C(1): 1.953(15), Au(2)–C(2): 2.005(13), Au(2)–C(3): 1.985(13), C(1)–N(1): 1.163(17), C(2)–N(2): 1.098(15), C(3)–N(3): 1.146(16).

The interactions between K$^+$ cations and $[AuI_2(CN)_2]^-$ anions in **3** are more complicated. As in **2**, the interactions are primarily with N(cyano) groups, with interaction distances of 2.824(15)–3.223(17) Å. However, some long K–I interactions ($d_{K–I}$ = 3.951(4)–4.094(4) Å; *cf.* $d_{K–I}$ = 3.52 Å for KI[56]) also exist, as shown in Fig. 5. This does not preclude the formation of I···I interactions, as only one out of three crystallographically unique iodide centres are bound to K$^+$ cations.

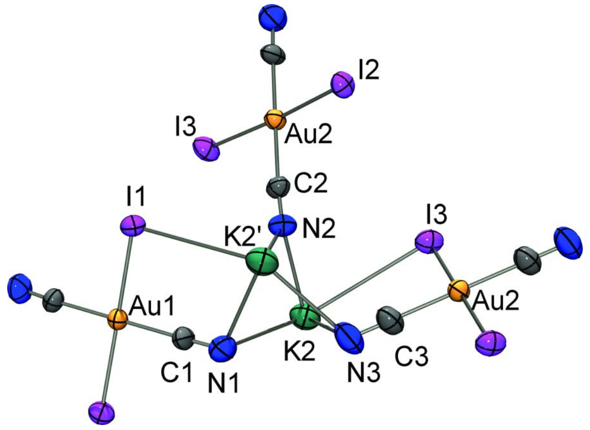

Fig. 5 Interactions between the K$^+$ cations and the iodo and cyano groups of the $[AuI_2(CN)_2]^-$ anions. Au, gold; I, violet; C, gray; N, blue; K, dark green. Selected bond lengths (Å): K(2)–I(1): 3.951(4), K(2)–I(3): 4.094(4), K(2)–N(1): 3.223(17), K(2)–N(2): 2.834(13), K(2)–N(3): 3.021(14).

The structural behaviour of these three salts clearly demonstrates the propensity of different halogens to form interactions with each other. An increase in the number of X···X interactions is seen moving from X = Cl to X = Br and I, where chains and triangles of interactions are seen, respectively. This behaviour is consistent with the increasing atomic radius and polarizability of the halogens,[22,57] and has been well studied from both an experimental and theoretical standpoint.[11,20,21]

3.2 Synthesis and crystal structures of mixed Au(I)/Au(III)-containing salts

In the above examples, it has been demonstrated that $[AuX_2(CN)_2]^-$ (X = Br, I) anions can aggregate *via* weak X···X interactions, despite electrostatic repulsion. However, no aurophilic Au^{III}···Au^{III} interactions were observed in any of the salts, consistent with the general absence of such interactions in the literature.[15,26,27] We thus targeted a mixed Au(I)/Au(III) system to examine the structural impact of introducing significant Au(I)-aurophilicity into the array. Hence, simple double salts containing a mixture of Au(I)-based $[Au(CN)_2]^-$ and Au(III)-based $[AuX_2(CN)_2]^-$ anions were prepared.

Slow evaporation of a methanol solution containing a nearly 1 : 1 mixture of K[Au(CN)$_2$] and K[AuBr$_2$(CN)$_2$] resulted in orange crystals of $K_3[Au(CN)_2]_2[AuBr_2(CN)_2]\cdot H_2O$ (**4**) alongside a yellow powder consisting of separately precipitated K[Au(CN)$_2$], K[AuBr$_2$(CN)$_2$] and AuCN (as confirmed by IR[17,44,58]). Crystals of **4** can also be obtained by slow evaporation of a stoichiometric solution, but in a much smaller yield. IR analysis of the crystals shows a weak ν_{CN} stretch at 2171 cm^{-1} and a strong ν_{CN} stretch at 2145 cm^{-1} corresponding to Au(III) and Au(I) anions, respectively.[48–50] Although small, the shift from 2176 cm^{-1} and 2142 cm^{-1} (the ν_{CN} stretches corresponding to the parent

Table 3 Selected interaction distances (Å) and angles (°) in **4** and **5**

Interaction distances (Å)		Interaction angles (°)	
$K_3[Au(CN)_2]_2[AuBr_2(CN)_2]\cdot H_2O$ (**4**)			
Au(2)–Au(2)[a]	3.2883(10)	Au(2)[a]–Au(2)–Au(3)	72.59(2)
Au(2)–Au(3)	3.4456(9)		
Au(3)–Au(3)[a]	3.3873(10)	Au(3)[a]–Au(3)–Au(2)	74.31(2)
Au(2)–Br(2)	3.2420(13)	Au(1)–Br(2)–Au(2)	175.60(5)
$K_5[Au(CN)_2]_4[AuI_2(CN)_2]\cdot 2H_2O$ (**5**)			
Au(1)–Au(2)	3.5796(5)	Au(2)–Au(1)–Au(2)[a]	179.997
Au(2)–Au(3)	3.4220(5)	Au(1)–Au(2)–Au(4)	111.276(13)
Au(2)–Au(4)	3.4454(5)	Au(3)–Au(2)–Au(4)	64.405(10)
Au(2)–I(1)	3.4518(10)	Au(2)–I(1)–Au(1)	158.74(5)

[a] Symmetry operation: $-x, -y, -z$.

$K[AuBr_2(CN)_2]$ and $K[Au(CN)_2]$ precursors, respectively[17,44]) is consistent with the presence of new crystallographic environments of the $[Au(CN)_2]^-$ and $[AuBr_2(CN)_2]^-$ units in **4**.

In a similar fashion to **2** and **3**, **4** forms layers of $[Au(CN)_2]^-$ and $[AuBr_2(CN)_2]^-$ anions separated by layers of K^+ cations. However, rather than being supported by a network of $X\cdots X$ (X = Br, I) interactions, these anions aggregate *via* both $Au^I\cdots Au^I$ and weak intermolecular $Au^I\cdots Br$ interactions (Table 3), yielding a square planar geometry for the Au(I) and Au(III) centres. As shown in Fig. 6, $Au^I\cdots Au^I$ interactions of 3.2883(10)–3.4456(9) Å lead to the formation of 1-D zig-zag chains of $[Au(CN)_2]^-$ anions. Pendant $[AuBr_2(CN)_2]^-$ units interact with these chains *via* intermolecular $Au^I\cdots Br$ interactions[59] of 3.2420(13) Å (*cf.* sum of van der Waals radii: 3.51 Å[22]). Such interactions have been observed in simple salts such as $Cs_2Au^IAu^{III}Br_6$, with d_{Au-Br} = 3.05–3.25 Å,[60] and have been claimed in some molecular structures such as $Au^I(PPh_3)$\{*bis*(4-Br-benzosulfonyl)amide\} with d_{Au-Br} = 3.597 Å.[61]

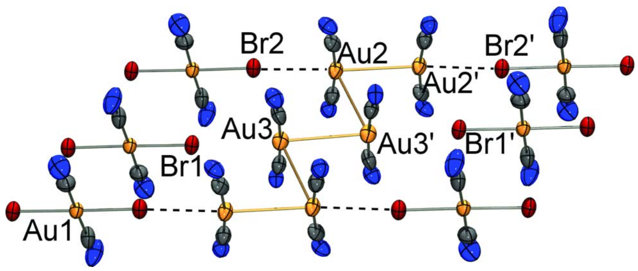

Fig. 6 1-D chains of **4** built up of $[Au(CN)_2]^-$ and $[AuBr_2(CN)_2]^-$ anions held together by a system of $Au^I\cdots Au^I$ and $Au^I\cdots Br$ interactions (K^+ cations and H_2O molecules removed for clarity; $Au^I\cdots Au^I$ interactions shown as yellow bonds, $Au^I\cdots Br$ interactions shown as dashed lines). Au, gold; Br, scarlet; C, gray; N, blue.

On the other hand, when a methanol solution containing a 4 : 1 mixture of $K[Au(CN)_2]$ and $K[AuI_2(CN)_2]\cdot\frac{1}{3}H_2O$ is allowed to slowly evaporate, red crystals of $K_5[Au(CN)_2]_4[AuI_2(CN)_2]\cdot 2H_2O$ (**5**) form alongside a brown powder consisting of separately precipitated $K[Au(CN)_2]$, $K[AuI_2(CN)_2]\cdot\frac{1}{3}H_2O$ and AuCN. Consistent with the presence of both Au(I) and Au(III) cyano groups, the IR spectrum shows ν_{CN} stretches shifted to 2168 cm^{-1} and 2144 cm^{-1} (corresponding to $[AuI_2(CN)_2]^-$ and $[Au(CN)_2]^-$, respectively). Other stoichiometries result in the same product, but in much lower yields.

X-Ray crystal structure analysis of **5** reveals another set of 2-D sheets of $[Au(CN)_2]^-$ and $[AuI_2(CN)_2]^-$ anions separated by layers of K^+ cations. In this case, the network is assembled mostly from $Au\cdots Au$ interactions (Table 3). Much like in **4**, zig-zag chains of $[Au(CN)_2]^-$ units connected by $Au^I\cdots Au^I$ interactions of 3.4220(5)–3.4454(5) Å form in one dimension, with each segment being made up of three $[Au(CN)_2]^-$ units. However, instead of having these chains connected by $Au\cdots I$ interactions in the other dimension (as in **4**), this is accomplished *via* rare, weak $Au^I\cdots Au^{III}$ interactions of 3.5796(5) Å, resulting in the overall 2-D structure seen in Fig. 7. Additional intermolecular $Au^I\cdots I$ interactions[59] of 3.4518(10) Å (*cf.* van der Waals radius: 3.64 Å[22]) can also be seen. Like the $Au^I\cdots Br$ interactions discussed earlier, $Au^I\cdots I$ interactions of 3.21–3.46 Å have also been previously observed in other simple salts such as $Cs_2Au^IAu^{III}I_6$.[62] These additional interactions do not increase dimensionality in this case, but lend support to the existing 2-D structure.

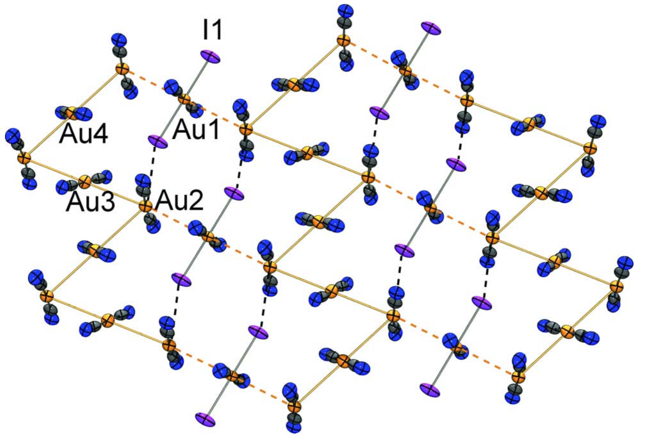

Fig. 7 2-D structure of **5** supported by $Au^I\cdots Au^I$, $Au^I\cdots I$ and $Au^I\cdots Au^{III}$ interactions (K^+ cations and H_2O molecules removed for clarity; $Au^I\cdots Au^I$ interactions shown as yellow bonds, $Au^I\cdots I$ interactions shown as black dashed lines and $Au^I\cdots Au^{III}$ interactions shown as yellow dashed lines). Au, gold; I, violet; C, gray; N, blue.

The K^+ cations in **4** and **5** play a very similar role to that in **1**, that is, they interact solely with the cyano groups of the $[Au(CN)_2]^-$ and $[AuX_2(CN)_2]^-$ anions, separating the anionic layers in the crystal structure (not shown). With interatomic K–N(cyano) distances of 2.918(12)–3.316(13) Å for **4** and 2.767(11)–3.074(11) Å for **5**, these are fairly strong interactions, consistent with the results of **1–3**.

In contrast to **4** and **5**, slow evaporation of a solution of $K[Au(CN)_2]$ and $K[AuCl_2(CN)_2]\cdot H_2O$ does not yield mixed salts containing both $[Au(CN)_2]^-$ and $[AuCl_2(CN)_2]^-$ anions, and simply results in the return of the $K[Au(CN)_2]$ and $K[AuCl_2(CN)_2]\cdot H_2O$ starting materials. This suggests that the propensity of the $[AuCl_2(CN)_2]^-$ anions to participate in $Au^I\cdots Cl$ or $Au^I\cdots Au^{III}$ interactions is very low, as it is through these types of interactions that the Au(III) anions aggregate with the Au(I) anions in **4** and **5**. With the $X\cdots X$ interaction trend observed with **1–3** (and in the literature),[18–21] it is clear that the size and polarizability of the halide ligand affects the propensity and strength of these interactions. The fact that $[Au(CN)_2]^-$ and $[AuCl_2(CN)_2]^-$ anions do not aggregate *via* these interactions is therefore consistent with this trend.

Although $Au\cdots X$ interactions are present in both **4** and **5** and undoubtedly play a role in the generation of the 2-D networks seen, the main factor holding the anions together is the presence of several Au···Au interactions. In both salts, chains of $[Au(CN)_2]^-$ anions are generated *via* well-known d^{10}–d^{10} aurophilic interactions. In the case of **4**, the Au(III)-containing $[AuBr_2(CN)_2]^-$ unit incorporates itself into the $[Au(CN)_2]^-$ network through $Au^I \cdots Br$ interactions. With **5**, however, the unusual $Au^I \cdots Au^{III}$ interaction is also seen. In the case of $Au^I \cdots Au^I$ interactions, theoretical studies (supported by experimental observations) have correlated the ancillary ligands on the Au(I) centre to the strength of the interaction.[27,63,64] Such studies suggest that softer, more polarizable ligands lead to an increased tendency to form aurophilic interactions, hence the $Au^I \cdots Au^{III}$ interactions are only seen with the softest of ligands here (X = I).

A noteworthy structural feature of **4** and **5** is the relative orientation of the cyano groups in pairs of $[Au(CN)_2]^-$ units. Whereas in **4** the *trans*-cyano groups of interacting Au(I) centres are parallel to each other, they are staggered in **5**. This reflects that such $Au^I \cdots Au^I$ interactions are rotationally flexible, with a very small energy difference between conformations.[2] The cyano groups in Au(I)/Au(III) pairs, however, are seen to always be nearly parallel. This may be related to the larger size of the iodo groups on the $[AuI_2(CN)_2]^-$ units.

The $Au^I \cdots Au^{III}$ distance of $d_{Au–Au} = 3.5796(5)$ Å suggests that it is likely much weaker than any of the $Au^I \cdots Au^I$ interactions present. Despite this, the few reported $Au^I \cdots Au^{III}$ interactions have only been observed either between cationic and anionic species,[34,35] such as in the aforementioned $[Au(C_{14}H_{22}N_4)][AuBr_2]$[35] or in a complex where proximity of the Au atoms is enforced by the ligand system,[32,33,38,39] such as $[S(Au_2dppf)\{Au(C_6F_5)_3\}_2]$[38] or $[Au(C_6F_5)_2\{PN(AuPPh_3)_2\}]ClO_4$[39] whereas in this case, two independent anions are held in proximity against their inherent electrostatic repulsion by a combination of $Au^I \cdots I$ and $Au^I \cdots Au^{III}$ interactions.

3.3 Emission properties of the mixed Au(I)/Au(III)-containing salts

One property of interest for $Au^I \cdots Au^I$ containing materials is their emission, which depends on the metal–metal distance.[15,30,31,65] Since both **4** and **5** have abundant $Au^I \cdots Au^I$ interactions, solid state emission measurements were conducted. However, in both cases, the compounds displayed no emission at room temperature despite the presence of these aurophilic interactions. This may be a result of $Au^I \cdots Au^{III}$ or $Au^I \cdots X$ interactions providing non-emissive pathways back to the ground state. There are virtually no experimental or theoretical studies of this issue to our knowledge.

4 Conclusions

The crystal structures of three dihalodicyanoaurate(III) salts were obtained and the propensity of the various halides to form X···X interactions were examined. In keeping with the trend of increasing van der Waals radii and polarizability going from Cl to Br to I, the number of such interactions also increased. In addition, two double salts containing cocrystallized $[Au(CN)_2]^-$ and $[AuX_2(CN)_2]^-$ anions were synthesized, showing similar 2-D motifs demonstrated by the $K[AuX_2(CN)_2]$ salts held together by a network of $Au^I \cdots X$ and Au···Au interactions. These structures demonstrate how influential such weak interactions can be in determining the overall structure, as well as their utility in structural design. Amongst these interactions was a rare $Au^I \cdots Au^{III}$ interaction.

In previous examples, proximity of the Au centres was enforced or encouraged either through a ligand framework or electrostatics. Here, such an interaction is found in **5** in the absence of strong supporting factors.

Finally, these building blocks provide opportunities to target new types of coordination polymers with increased structural dimensionality with the assistance of weak Au···Au, Au···X and X···X interactions, an avenue which we are currently exploring.

Acknowledgements

The authors thank NSERC of Canada and Natural Resources Canada (JSO) for financial support.

References

1 J. D. Dunitz and A. Gavezzotti, *Chem. Soc. Rev.*, 2009, **38**, 2622.
2 H. Schmidbaur and A. Schier, *Chem. Soc. Rev.*, 2012, DOI: 10.1039/c1cs15182g, Advanced Article.
3 C. Janiak, *Dalton Trans.*, 2003, 2781.
4 S. Sculfort and P. Braunstein, *Chem. Soc. Rev.*, 2011, **40**, 2741.
5 G. R. Desiraju, *Angew. Chem., Int. Ed.*, 2007, **46**, 8342.
6 H.-J. Schneider and A. K. Yatsimirsky, *Chem. Soc. Rev.*, 2008, **37**, 263.
7 M. Roman, C. Cannizzo, T. Pinault, B. Isare, B. Andrioletti, P. van der Schoot and L. Bouteiller, *J. Am. Chem. Soc.*, 2010, **132**, 16818.
8 R. D. Poulsen, J. Overgaard, A. Schulman, C. Østergaard, C. A. Murillo, M. A. Spackman and B. B. Iversen, *J. Am. Chem. Soc.*, 2009, **131**, 7580.
9 S. Sato, O. Morohara, D. Fujita, Y. Yamaguchi, K. Kato and M. Fujita, *J. Am. Chem. Soc.*, 2010, **132**, 3670.
10 I. Chung, J.-H. Song, J. I. Jang, A. J. Freeman, J. B. Ketterson and M. G. Kanatzidis, *J. Am. Chem. Soc.*, 2009, **131**, 2647.
11 O. Navon, J. Bernstein and V. Khodorkovsky, *Angew. Chem., Int. Ed. Engl.*, 1997, **36**, 601.
12 P.-P. Zhang, J. Peng, H.-J. Pang, J.-Q. Sha, M. Zhu, D.-D. Wang, M.-G. Liu and Z.-M. Su, *Cryst. Growth Des.*, 2011, **11**, 2736.
13 B. Ji, W. Wang and D. Dongsheng, *Cryst. Growth Des.*, 2011, **11**, 3622.
14 M. J. Katz, H. Kaluarachchi, R. J. Batchelor, G. Schatte and D. B. Leznoff, *Cryst. Growth Des.*, 2007, **7**, 12.
15 M. J. Katz, K. Sakai and D. B. Leznoff, *Chem. Soc. Rev.*, 2008, **37**, 1884.
16 J. S. Ovens, A. R. Geisheimer, A. A. Bokov, Z.-G. Ye and D. B. Leznoff, *Inorg. Chem.*, 2010, **49**, 9609.
17 J. S. Ovens and D. B. Leznoff, *Dalton Trans.*, 2011, **40**, 4140.
18 D. M. Bassani, L. Jonusauskaite, A. Lavie-Cambot, N. D. McClenaghan, J.-L. Pozzo, D. Ray and G. Vives, *Coord. Chem. Rev.*, 2010, **254**, 2429.
19 P. Metrangolo, G. Resnati, T. Pilati and S. Biella, *Struct. Bonding*, 2008, **126**, 105.
20 F. F. Awwadi, R. D. Willett, K. A. Peterson and B. Twamley, *Chem.–Eur. J.*, 2006, **12**, 8952.
21 G. Desiraju and R. Parthasarathy, *J. Am. Chem. Soc.*, 1989, **111**, 8725.
22 A. Bondi, *J. Phys. Chem.*, 1964, **68**, 441.
23 M. Bardají and A. Laguna, *Eur. J. Inorg. Chem.*, 2003, 3069.
24 Q.-J. Pan, X. Zhou, Y.-R. Guo, H.-G. Fu and H.-X. Zhang, *Inorg. Chem.*, 2009, **48**, 2844.
25 J. R. Stork, M. M. Olmstead and A. L. Balch, *J. Am. Chem. Soc.*, 2005, **127**, 6512.
26 P. Pyykkö, *Chem. Rev.*, 1997, **97**, 597.
27 P. Pyykkö, *Angew. Chem., Int. Ed.*, 2004, **43**, 4412.
28 V. Phillips, F. G. Baddour, T. Lasanta, J. M. López-de Luzuriaga, J. W. Bacon, J. A. Golen, A. L. Rheingold and L. H. Doerrer, *Inorg. Chim. Acta*, 2010, **364**, 195.
29 S. J. Ludy, C. P. Landee, M. M. Turnbull and J. L. Wikaira, *J. Coord. Chem.*, 2011, **64**, 134.
30 H. Schmidbaur and A. Schier, *Chem. Soc. Rev.*, 2008, **37**, 1931.

31 M. Katz, T. Ramnial, H. Yu and D. Leznoff, *J. Am. Chem. Soc.*, 2008, **130**, 10662.

32 M. A. Bennett, D. C. R. Hockless, A. D. Rae, L. L. Welling and A. C. Willis, *Organometallics*, 2001, **20**, 79.

33 R. G. Raptis, L. C. Porter, R. J. Emrich, H. H. Murray and J. P. Fackler Jr., *Inorg. Chem.*, 1990, **29**, 4408.

34 L. Cao, M. C. Jennings and R. J. Puddephatt, *Inorg. Chem.*, 2007, **46**, 1361.

35 V. A. Afanas'eva, L. A. Glinskaya, R. F. Klevtsova and I. V. Mironov, *Russ. J. Coord. Chem.*, 2011, **37**, 325.

36 R. Hayoun, D. K. Zhong, A. L. Rheingold and L. H. Doerrer, *Inorg. Chem.*, 2006, **45**, 6120.

37 T. M. Klaptke, B. Krumm, J. C. Galvez-Ruiz and H. Noth, *Inorg. Chem.*, 2005, **44**, 9625.

38 F. Canales, M. C. Gimeno, A. Laguna and P. G. Jones, *Organometallics*, 1996, **15**, 3412.

39 E. J. Fernández, M. Gil, M. E. Olmos, O. Crespo, A. Laguna and P. G. Jones, *Inorg. Chem.*, 2001, **40**, 3018.

40 S. Canales, O. Crespo, M. C. Gimeno, P. G. Jones and A. Laguna, *Inorg. Chem.*, 2004, **43**, 7234.

41 K. Ortner, L. Hilditch, Y. F. Zheng, J. R. Dilworth and U. Abram, *Inorg. Chem.*, 2000, **39**, 2801.

42 F. Mendizabal and P. Pyykkö, *Phys. Chem. Chem. Phys.*, 2004, **6**, 900.

43 F. Mendizabal, G. Zapata-Torres and C. Olea-Azar, *Chem. Phys. Lett.*, 2003, **382**, 92.

44 J. M. Smith, L. H. Jones, I. K. Kressin and R. A. Penneman, *Inorg. Chem.*, 1965, **4**, 369.

45 P. W. Betteridge, J. R. Carruthers, R. I. Cooper, K. Prout and D. J. Watkin, *J. Appl. Crystallogr.*, 2003, **36**, 1487.

46 L. J. Farrugia, *J. Appl. Crystallogr.*, 1997, **30**, 565.

47 T. D. Fen, D. Ringe and G. A. Petsko, *J. Appl. Crystallogr.*, 2003, **36**, 944.

48 L. Jones, *Inorg. Chem.*, 1964, **3**, 1581.

49 C. J. Shorrock, H. Jong, R. J. Batchelor and D. B. Leznoff, *Inorg. Chem.*, 2003, **42**, 3917.

50 P. Vitoria, J. M. Gutie, A. Luque, P. Roma, L. Lezama, F. J. Zu, J. I. Beitia, M. Condensada, F. D. Ciencias, U. Pa and E. Bilbao, *Inorg. Chem.*, 2003, **42**, 960.

51 T. S. Teets and D. G. Nocera, *J. Am. Chem. Soc.*, 2009, **131**, 7411.

52 M. J. Katz and D. B. Leznoff, *J. Am. Chem. Soc.*, 2009, **131**, 18435.

53 S. D. Khanye, N. B. Báthori, G. S. Smith and K. Chibale, *Dalton Trans.*, 2010, **39**, 2697.

54 D. L. Price, J. M. Rowe, J. J. Rush, E. Prince, D. G. Hinks and S. Susman, *J. Chem. Phys.*, 1972, **56**, 3697.

55 V. L. Cherginets, V. N. Baumer, S. S. Galkin, L. V. Glushkova, T. P. Re-brova and Z. V. Shtitelman, *Inorg. Chem.*, 2006, **45**, 7367.

56 P. Cortona, *Phys. Rev. B: Condens. Matter*, 1992, **46**, 2008.

57 *CRC Handbook of Chemistry and Physics*, ed. D. R. Lide, CRC Press, Inc., Boca Raton, FL, 71st edn, 1990.

58 G. A. Bowmaker, B. J. Kennedy and J. C. Reid, *Inorg. Chem.*, 1998, **37**, 3968.

59 I. A. Baidina and E. V. Makotchenko, *J. Struct. Chem.*, 2010, **51**, 192.

60 N. Matsushita, F. Fukuhara and N. Kojima, *Acta Crystallogr., Sect. E: Struct. Rep. Online*, 2005, **61**, i123.

61 C. Wölper, S. Roca Piñol, S. Durán Ibáñez, M. Freytag, P. G. Jones and A. Blaschette, *Z. Anorg. Allg. Chem.*, 2008, **634**, 1506.

62 N. Matsushita, H. Kitagawa and N. Kojima, *Acta Crystallogr., Sect. C: Cryst. Struct. Commun.*, 1997, **53**, 663.

63 P. Van Calcar, M. Olmstead and A. Balch, *Inorg. Chem.*, 1997, **36**, 5231.

64 P. Pyykkö, N. Runeberg and F. Mendizabal, *Chem.–Eur. J.*, 1997, **3**, 1451.

65 O. Elbjeirami, M. W. A. Gonser, B. N. Stewart, A. E. Bruce, M. R. M. Bruce, T. R. Cundari and M. A. Omary, *Dalton Trans.*, 2009, 1522.